Microscopic model of critical current noise in Josephson-junction qubits: Subgap resonances and Andreev bound states

Rogério de Sousa,[1] K. Birgitta Whaley,[2] Theresa Hecht,[3] Jan von Delft,[3] and Frank K. Wilhelm[4]
[1]*Department of Physics and Astronomy, University of Victoria, Victoria, British Columbia, Canada V8V 4H3*
[2]*Department of Chemistry and Pitzer Center for Theoretical Chemistry, University of California, Berkeley, California 94720-1460, USA*
[3]*Physik Department, CeNS, and ASC, Ludwig-Maximilians-Universität, Theresienstr. 37, D-80333 München, Germany*
[4]*Department of Physics and Astronomy and Institute for Quantum Computing, University of Waterloo, 200 University Avenue W, Waterloo, Ontario, Canada N2L 3G1*
(Received 28 June 2009; published 18 September 2009)

We propose a microscopic model of critical current noise in Josephson junctions based on individual trapping centers in the tunnel-barrier hybridized with electrons in the superconducting leads. We calculate the noise exactly in the limit of no on-site Coulomb repulsion. Our result reveals a noise spectrum that is dramatically different from the usual Lorentzian assumed in simple models. We show that the noise is dominated by sharp subgap resonances associated to the formation of pairs of Andreev bound states, thus providing a possible explanation for the spurious two-level systems (microresonators) observed in Josephson-junction qubits [R. W. Simmonds *et al.*, Phys. Rev. Lett. **93**, 077003 (2004).]. Another implication of our model is that each trapping center will contribute a sharp dielectric resonance only in the superconducting phase, providing an effective way to validate our results experimentally. We derive an effective Hamiltonian for a qubit interacting with Andreev bound states, establishing a direct connection between phenomenological models and the microscopic parameters of a Fermionic bath.

DOI: 10.1103/PhysRevB.80.094515 PACS number(s): 74.50.+r, 74.40.+k

I. INTRODUCTION

The performance of Josephson-junction devices functioning as units of quantum memory or as qubits depends to a large extent on the amount of charge and critical current noise affecting each Josephson junction.[1–3] One mechanism for critical current noise is to assume that trapping centers (TCs) located in the tunnel barrier will partially block conduction whenever they capture electrons from one of the superconducting electrodes [Fig. 1(a)].[4] The noise resulting from each TC is traditionally modeled as two-level telegraph noise, with a Lorentzian noise spectrum, and a combination of several TCs leads to $1/f$ noise.[5]

Nevertheless, sensitive spectroscopy experiments on current-biased Josephson junctions (phase qubits) revealed the presence of a few microwave resonators on top of the expected $1/f$ noise.[6] These microresonators behave as spurious two-level systems buried within the tunnel barrier, whose coupling to the qubit produces reduced measurement fidelity and decoherence.[7] Similar microresonators were observed in flux qubits.[8] The microscopic origin of the microresonator remains unknown. However, there is strong evidence that improving the junction oxide quality reduces their concentration.[9] Recently, phenomenological models based on resonant coupling with the Josephson energy[6] and dielectric resonance[10] were proposed. Two measurement schemes to distinguish these different models were suggested.[11,12] An interesting connection between the low- and high-frequency scales of the noise spectrum due to a large number of microresonators was demonstrated.[13] To our knowledge, there are two proposals in the literature for the microscopic origin of these microresonators. The first is based on macroscopic resonant tunneling in large Josephson junctions.[14] This model explains the splitting of the Josephson energy but predicts no dielectric resonance for the microresonator. The second microscopic model is based on the structural two-level system in glasses.[10,15] This gives rise to the *same* dielectric resonance above and below the superconducting critical temperature. Recently, a quantum computer architecture using microresonators as qubits was proposed.[16] Therefore, understanding the microscopic origin of the microresonator is of central importance for improving superconducting qubits.

In a previous paper, we studied the charge noise spectrum due to a single TC hybridized with a nonsuperconducting Fermi sea.[17] At high temperatures we showed that the presence of a single TC with energy level close to the Fermi level leads to the expected Lorentzian spectrum characteristic of semiclassical random telegraph noise. At lower temperatures and frequencies below the TC linewidth, the noise has a

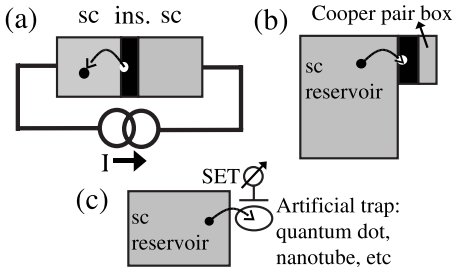

FIG. 1. (a) A current-biased Josephson junction adversely affected by the tunneling of electrons between one of the superconducting leads (sc) and a trapping-center defect in the insulating barrier (ins.). Josephson-junction critical current noise is directly related to fluctuations in trapping-center occupation due to modulation of the tunneling rate between superconducting leads. (b) A Cooper-pair box quantum bit affected by charge noise produced by a single trapping center in the barrier. (c) Proposed setup for measuring trap noise close to the superconducting transition. A single-electron transistor (SET) is weakly coupled to an artificial trap, e.g., a normal-state quantum dot or a nanotube.

quantum Johnson-Nyquist form reflecting the electron-hole excitations in the gate electrode Fermi sea.[17]

Here we consider the noise spectrum due to a single TC hybridized with electrons in a superconductor. We show that the noise spectrum of each TC is characterized by a sharp resonance associated to the Andreev bound states formed from the TC hybridization with the superconductor. We further demonstrate that our theory describes a direct connection between this TC physics and the spurious microresonators observed at subgap frequencies in Josephson-junction devices.[6–8] We derive an effective Hamiltonian connecting the discrete levels to the microscopic parameters of the TC plus superconductor bath. Since the TC has an electric dipole moment, our model predicts that a sharp dielectric resonance will appear when the sample becomes superconducting.

The model proposed here is based on tunneling events between *individual* TCs and the superconductor. This is different from other models[18–20] that considered charge tunneling between two TCs mediated by Andreev states, resulting in a smooth noise spectrum that does not give rise to microresonators.

Trapping-center fluctuation nearby to single-electron tunneling devices[21] is also an important source of charge noise and decoherence of charge qubits such as the Cooper-pair box[22,23] [Fig. 1(b)] and double quantum dot.[24] Figure 1(c) suggests a test device to probe TC noise around the superconducting transition temperature T_c that allows verification of our predictions in a controlled manner. A tunable artificial trap, which can be realized by a quantum dot or a nanotube in the normal state,[25] is coupled to a large metallic reservoir at temperatures close to the superconducting transition. A single-electron transistor (SET) is proposed to measure TC charge occupation in real time.[26] This will map the emergence of the subgap resonance as T is lowered below the superconducting transition temperature T_c.

II. QUBIT DECOHERENCE AND QUANTUM NOISE

The behavior of superconducting circuits containing Josephson junctions is markedly quantum mechanical. Hence one can design circuits that behave as artificial two-level systems, realizing promising qubits for scalable quantum computer architectures.[27]

Consider a model for an artificial two-level system,

$$\mathcal{H}_{\text{Qubit}} = \frac{1}{2}\hbar \mathbf{\Omega}(\hat{I}_c)\cdot \hat{\boldsymbol{\sigma}}, \tag{1}$$

where $\hat{\boldsymbol{\sigma}}=(\hat{\sigma}_x,\hat{\sigma}_y,\hat{\sigma}_z)$ is the vector of Pauli matrices denoting the qubit and $\mathbf{\Omega}$ is a vector with dimensions of frequency. The latter is a function of $\hat{I}_c$, the critical current of one of the Josephson junctions in the circuit. We assume the critical current depends on the quantum state of TCs in the barrier, hence we write it as an operator (notation $\hat{I}_c$ to distinguish quantum operators from c numbers such as I_c). For small fluctuations we may write $\mathbf{\Omega}(\hat{I}_c)\approx \mathbf{\Omega}_0+\mathbf{\Omega}_0'(\delta\hat{I}_c)+\mathcal{O}(\delta\hat{I}_c)^2$, where $\mathbf{\Omega}_0=\mathbf{\Omega}(\langle\hat{I}_c\rangle)$ and $(\delta\hat{I}_c)=\hat{I}_c-\langle\hat{I}_c\rangle$. Choosing a coordinate system with z axis along $\mathbf{\Omega}_0$, and x axis along $\mathbf{\Omega}_1=\mathbf{\Omega}_0'-(\mathbf{\Omega}_0'\cdot\hat{z})\hat{z}$ we get

$$\mathcal{H}_{\text{Qubit}} = \frac{1}{2}\hbar\Omega_0\hat{\sigma}_z + \hbar\eta_z(\delta\hat{I}_c)\hat{\sigma}_z + \hbar\eta_x(\delta\hat{I}_c)\hat{\sigma}_x. \tag{2}$$

Fluctuations in $\delta\hat{I}_c$ affects the qubit through the parameters $\eta_z=\frac{1}{2}\mathbf{\Omega}_0'\cdot\hat{z}$ and $\eta_x=\frac{1}{2}\Omega_1$. The former leads to phase relaxation or decoherence while the latter causes energy relaxation.

In the weak-coupling regime, all relaxation effects are fully characterized by the critical current noise spectrum,

$$\tilde{S}_I(\omega) = \int_{-\infty}^{\infty}\frac{dt}{2\pi}e^{i\omega t}\langle[\hat{I}_c(t)-\langle\hat{I}_c\rangle][\hat{I}_c(0)-\langle\hat{I}_c\rangle]\rangle. \tag{3}$$

For example, if the qubit is prepared in the excited state ($|\uparrow\rangle$), its rate of approach toward thermal equilibrium will be given by

$$\frac{1}{T_1} = \frac{\pi}{2}\eta_x^2[\tilde{S}(\Omega_0)+\tilde{S}(-\Omega_0)]. \tag{4}$$

Similarly, if the qubit is prepared in a superposition state $(|\uparrow\rangle+|\downarrow\rangle)/\sqrt{2}$, its coherence envelope $\langle\hat{\sigma}_+\rangle=\langle\hat{\sigma}_x+i\sigma_y\rangle$ will be affected by low-frequency noise according to[28,29]

$$|\langle\sigma_+(t)\rangle| = \exp\left[-\eta_z^2\int_{-\infty}^{\infty}d\omega\tilde{S}_I(\omega)\mathcal{F}(t,\omega)\right]. \tag{5}$$

Here the filter function $\mathcal{F}(t,\omega)$ depends on the particular method chosen for probing qubit coherence. For free induction decay we have

$$\mathcal{F}_{\text{FID}}(t,\omega) = \frac{1}{2}\frac{\sin^2(\omega t/2)}{(\omega/2)^2}, \tag{6}$$

while for the Hahn echo

$$\mathcal{F}_{\text{Hahn}}(2t_e,\omega) = \frac{1}{2}\frac{\sin^4(\omega t_e/2)}{(\omega/4)^2}, \tag{7}$$

with qubit coherence probed at $t=2t_e$ after the application of a π pulse at time t_e. Note that $\mathcal{F}_{\text{Hahn}}(2t_e,0)=0$. The Hahn echo filters out terms proportional to $\tilde{S}_I(0)$ hence leading to much longer coherence times for qubits subject to low-frequency noise (see Ref. 29 for further discussion and derivations).

For the purposes of this work, it is instructive to use Eq. (5) to study the effect of a sharp frequency peak (a resonance) in the noise spectrum. Assume $\tilde{S}_I(\omega)$ has a sharp peak centered at Ω_{Res} with linewidth $1/\tau_d$,

$$\tilde{S}_I(\omega) = \frac{\tau_d}{\pi}\frac{1}{(\omega-\Omega_{\text{Res}})^2\tau_d^2+1}. \tag{8}$$

Using Eqs. (5) and (6) and assuming $\Omega_{\text{Res}}\gg 1/\tau_d$ we get

$$|\langle\sigma_+(t)\rangle| \approx \exp\left[-2\left(\frac{\eta_z}{\Omega_{\text{Res}}}\right)^2(1-e^{-t/\tau_d}\cos\Omega_{\text{Res}}t)\right]. \tag{9}$$

Therefore a resonance in the noise spectrum leads to loss of visibility of coherence oscillations. The loss of visibility is initially oscillatory but decays exponentially to a fixed contrast for $t\gg\tau_d$, similar to Ref. 30. Although Eq. (9) was cal-

culated for free induction decay, it is also a good approximation for Hahn echoes in the limit $\Omega_{\mathrm{Res}} \gg 1/t_e$.

The above discussion makes clear the fact that the key quantity to be studied in the context of qubit relaxation and decoherence is the time-ordered noise spectrum defined by Eq. (3). If noise is the object of interest, the qubit acts as a spectrometer for quantum noise.[31] Later, in Sec. VII we are going to show that the same basic Hamiltonian also leads to the formation of avoided crossing with Andreev levels acting as junction resonators.

III. MICROSCOPIC MODEL FOR CRITICAL CURRENT NOISE

A. Trapping-center model Hamiltonian

The Hamiltonian for a trapping center coupled to a lead with Bardeen-Cooper-Schrieffer (BCS) interactions is given by[32,33]

$$\mathcal{H} = \mathcal{H}_0 + \mathcal{H}_{\mathrm{BCS}} + \mathcal{V}. \tag{10}$$

The unperturbed trap Hamiltonian reads

$$\mathcal{H}_0 = \sum_{\sigma} \epsilon_d n_{\sigma}, \tag{11}$$

where $n_\sigma = d_\sigma^\dagger d_\sigma$ is the electron number operator for a TC with spin $\sigma = \uparrow, \downarrow$ and $d_\sigma^\dagger$ is a Fermion creation operator. The trap-energy level ϵ_d is measured with respect to the Fermi level (we assume $\epsilon_F = 0$). The unperturbed mean-field Hamiltonian for a superconducting Fermi lead is given by

$$\mathcal{H}_{\mathrm{BCS}} = \sum_{k,\sigma} \epsilon_k n_{k\sigma} - \sum_k \Delta c_{k\uparrow}^\dagger c_{-k\downarrow}^\dagger + \mathrm{H.c}, \tag{12}$$

where $c_{k\sigma}^\dagger$ creates a conduction electron in the gate electrode with energy ϵ_k and $n_{k\sigma} = c_{k\sigma}^\dagger c_{k\sigma}$. Δ is the superconducting order parameter. The conduction electrons are hybridized with the TC via the hopping Hamiltonian

$$\mathcal{V} = \sum_{k,\sigma} V_k d_\sigma^\dagger c_{k\sigma} + \mathrm{H.c}, \tag{13}$$

where V_k is the tunneling matrix element for the electron between the TC and the superconducting lead.

Here we assume TCs for which the on-site Coulomb repulsion of the form $U n_\uparrow n_\downarrow$ can be neglected. We remark that the chemical structure of TCs in the Josephson barrier is not known. There are many possible kinds of TCs associated with the amorphous oxide in a typical Josephson junction: O-H complexes, various kinds of vacancies, dangling bonds, etc. Our model will be applicable to TCs with $U \ll \Delta$. The $U=0$ idealization is an important starting point, *particularly because it allows an exact solution of the noise problem*. As we show below, our model seems to explain some of the important features observed in spectroscopy of Josephson qubits. In Sec. VIII we discuss the expected modifications when $U > 0$.

B. Trapping-center fluctuation as a mechanism for critical current noise

We now describe a model for the effect of TC fluctuation on the critical current of a Josephson junction [Fig. 1(a)]. Our aim is to establish a direct relationship between critical current noise and the TC noise spectrum

$$\tilde{S}_n(\omega) = \int_{-\infty}^{\infty} \frac{dt}{2\pi} e^{i\omega t} \langle [\hat{n}(t) - 2\bar{n}][\hat{n}(0) - 2\bar{n}] \rangle. \tag{14}$$

Here $\hat{n} = \Sigma_\sigma d_\sigma^\dagger d_\sigma$ is the total number operator for electrons occupying the TC level. The notation $\langle \hat{A} \rangle = \mathrm{Tr}\{\hat{\rho}_G \hat{A}\}$ denotes grand-canonical averages using the density operator $\hat{\rho}_G = e^{-\beta(\mathcal{H}-\mu N)}/Z_G$, with $\beta = 1/k_B T$ and Z_G the grand-canonical partition function. In the absence of a magnetic field, $\langle \hat{n}_\uparrow \rangle = \langle \hat{n}_\downarrow \rangle \equiv \bar{n}$, therefore we write $\langle \hat{n} \rangle = 2\bar{n}$ to simplify the notation.

The presence of a TC will produce weak modulations on the junction potential barrier.[1,4,15] Our model is to assume that the channel average matrix element for electrons tunneling from one lead to the other depends on $\hat{n}$ according to

$$\hat{T}_{LR} \approx T_{LR}^{(0)} + T_{LR}^{(1)} \hat{n}. \tag{15}$$

The critical current $\hat{I}_c$ [or equivalently, the Josephson energy $\hat{E}_J = (\hbar/2e)\hat{I}_c$] is proportional to the modulus squared of Eq. (15),[34] so that in the adiabatic limit, for frequencies smaller than the inverse tunneling time,[35] this directly translates into a fluctuation of the critical current

$$\hat{I}_c \approx I_{0c} \left(1 + \frac{|T_{LR}^{(1)}|}{|T_{LR}^{(0)}|} \hat{n} \right). \tag{16}$$

The critical current noise is therefore given by

$$\tilde{S}_I(\omega) = \frac{I_{c0}^2 |T_{LR}^{(1)}|^2}{|T_{LR}^{(0)}|^2} \int_{-\infty}^{\infty} \frac{dt}{2\pi} e^{i\omega t} \langle [\hat{n}(t) - 2\bar{n}][\hat{n}(0) - 2\bar{n}] \rangle$$

$$= (\delta I_c)^2 \tilde{S}_n(\omega). \tag{17}$$

Hence within the linear approximation [Eq. (15)] the resulting critical current noise is directly proportional to the TC charge noise, $\tilde{S}_n(\omega)$. The proportionality constant can be extracted directly from experiments probing critical current noise.[2,4,36] Below we focus on theoretical calculations of the TC noise spectrum $\tilde{S}_n(\omega)$ under different parameter regimes.

Our model assumes the TC is coupled to only one of the superconducting leads. Within the one-lead approximation critical current modulations are assumed to occur only through variations in interlead tunneling due to population/depopulation of the trap [Eq. (15)]. We therefore neglect the possibility for the trap electron to enter through one lead and exit through the other. These processes will lead to interesting phase-dependent effects in the Josephson current.[37,38] We are not aware of studies of critical current noise in this regime. Nevertheless, for zero phase difference between the leads, we may map the problem into a TC coupled to a single lead.[38] Therefore our results should remain valid in this case provided the phase is set to zero. In an experimental sample containing a few TCs we should expect that some of these are coupled to a single lead, others are coupled to both leads. The former case will lead to phase-independent noise while the latter is expected to generate a phase-dependent noise spectrum. In this context the theory developed here should

be compared to measurements of the *phase-independent contributions to critical current noise*.[2] Note that the TC only couples to both leads if it is in the middle of the junction with a difference in separations to either lead being smaller than a tunnel length. Given that junctions are typically much thicker than a tunneling length to the extent that the latter are known,[39] the present theory covers most of the possible TC locations.

In this work we calculate the noise spectrum under the assumption that the TC remains in thermal equilibrium with the superconducting reservoir. Therefore our results are valid at the regime where nonequilibrium effects are weak or can be neglected. This is the case for a current-biased Josephson junction in the zero-voltage state or whenever the voltage is low enough so that the electrons in the lead may still be characterized by a Fermi distribution. The thermal equilibrium assumption implies that the noise spectrum satisfies the detailed balance condition, $\tilde{S}(-\omega)=e^{-\hbar\omega/k_BT}\tilde{S}(\omega)$. The finite frequency noise spectrum measured by a particular detector depends on details such as the detector temperature T_D (not necessarily equal to the TC plus Fermi sea temperature T). For example, current noise measured by an LC circuit relates to our calculated time-ordered noise [Eq. (17)] in the following way[40]

$$\tilde{S}_I^{(\mathrm{LC})}(\omega)=K\left\{\tilde{S}_I(-\omega)+\frac{1}{e^{\hbar\omega/k_BT_D}-1}[\tilde{S}_I(-\omega)-\tilde{S}_I(\omega)]\right\}, \tag{18}$$

where K denotes the effective coupling constant between the current-carrying wire and the LC circuit. The experiment proposed in Fig. 1(c) should be interpreted using Eq. (18).

IV. RELATIONSHIP BETWEEN NOISE AND TRAPPING-CENTER SPECTRAL FUNCTIONS

In this section we show that the TC noise spectrum, Eq. (14), can be expressed as an integral over all possible quasiparticle-quasihole excitations in the TC plus superconductor problem. In order to derive this result, we define the Matsubara and real-time correlation functions as follows:[41]

$$\mathcal{S}(\tau-\tau')=-\mathrm{Tr}\{\hat{\rho}_G\hat{T}_\tau[\delta\hat{n}(\tau)\delta\hat{n}(\tau')]\}, \tag{19a}$$

$$S^{(R)}(t-t')=-i\theta(t-t')\mathrm{Tr}\{\hat{\rho}_G[\delta\hat{n}(t),\delta\hat{n}(t')]\}, \tag{19b}$$

where we used the notation $\delta\hat{n}\equiv\hat{n}-2\bar{n}$. Here, we use the Matsubara representation of operators $\hat{n}(\tau)=e^{\tau\mathcal{H}/\hbar}\hat{n}(0)e^{-\tau\mathcal{H}/\hbar}$, that are obtained from the Heisenberg representation by substituting $it\to\tau$.

Applying Wick's theorem to Eq. (19a) leads to

$$\mathcal{S}(\tau)=\sum_{\sigma,\sigma'}[\mathcal{G}_{\sigma\sigma'}(\tau)\mathcal{G}_{\sigma'\sigma}(-\tau)-\mathcal{F}^\dagger_{\sigma'\sigma}(\tau)\mathcal{F}_{\sigma'\sigma}(-\tau)], \tag{20}$$

where we have introduced the normal $\mathcal{G}$ and anomalous $\mathcal{F}$ TC Matsubara Green's functions,

$$\mathcal{G}_{\sigma\sigma'}(\tau)=-\mathrm{Tr}\{\hat{\rho}_G\hat{T}_\tau[d_\sigma(\tau)d^\dagger_{\sigma'}(0)]\}, \tag{21a}$$

$$\mathcal{F}_{\sigma\sigma'}(\tau)=-\mathrm{Tr}\{\hat{\rho}_G\hat{T}_\tau[d_\sigma(\tau)d_{\sigma'}(0)]\}. \tag{21b}$$

We now take the Fourier transform of Eq. (20), $\tilde{S}(i\omega_n)=\int_0^{\beta\hbar}d\tau e^{i\omega_n\tau}\mathcal{S}(\tau)$, and insert the Lehmann representation for the TC Green's functions,

$$\mathcal{G}_{\sigma\sigma'}(i\omega_n)=\hbar\int_{-\infty}^{\infty}d\omega'\frac{\mathcal{A}_{\sigma\sigma'}(\omega')}{i\omega_n-\omega'}, \tag{22a}$$

$$\mathcal{F}_{\sigma\sigma'}(i\omega_n)=\hbar\int_{-\infty}^{\infty}d\omega'\frac{\mathcal{B}_{\sigma\sigma'}(\omega')}{i\omega_n-\omega'}. \tag{22b}$$

The TC spectral functions $\mathcal{A}_{\sigma\sigma'}(\omega)$ and $\mathcal{B}_{\sigma\sigma'}(\omega)$ play a fundamental role in our theory. For a BCS model such as Eq. (10), we have $\mathcal{A}_{\uparrow\uparrow}=\mathcal{A}_{\downarrow\downarrow}\equiv\mathcal{A}$ with $\mathcal{A}$ real and $\mathcal{A}_{\uparrow\downarrow}=\mathcal{A}_{\downarrow\uparrow}=0$. Also, the spectral function related to Gorkov's $\mathcal{F}$ function is nonzero only for $\mathcal{B}_{\uparrow\downarrow}=\mathcal{B}_{\downarrow\uparrow}\equiv\mathcal{B}$, with $\mathcal{B}$ real. After inserting these Lehmann representations into Eq. (20), the result is readily evaluated using the residue theorem, and taking advantage of the fact that $\tilde{S}(i\omega_n)$ is nonzero only at even (Bose) Matsubara frequencies [$\omega_n=n\pi/(\hbar\beta)$ with n even]. Finally, analytic continuation ($i\omega_n\to\omega+i\eta$) allows us to extract the TC noise spectrum from the imaginary part of $\tilde{S}^{(R)}(\omega)$. This leads to a convenient expression for the TC noise spectrum,

$$\tilde{S}_n(\omega)=\hbar\sum_{\sigma\sigma'}\int_{-\infty}^{\infty}d\epsilon'[\mathcal{A}_{\sigma\sigma'}(\epsilon')\mathcal{A}_{\sigma\sigma'}(\epsilon'-\omega) - \mathcal{B}^*_{\sigma'\sigma}(\epsilon')\mathcal{B}_{\sigma'\sigma}(\epsilon'-\omega)][1-f(\epsilon')]f(\epsilon'-\omega). \tag{23}$$

Here the Fermi functions are given by

$$f(\epsilon)=\frac{1}{e^{\beta\epsilon}+1}. \tag{24}$$

The expression (23) is an exact result. Its derivation relied on the use of Wick's theorem, which is valid only for a quadratic Hamiltonian (10) ($U=0$).[41] It expresses the fact that the TC noise spectrum is the sum of all quasiparticle-quasihole excitations involving the dressed TC plus superconductor at thermal equilibrium. Equation (23) is the generalization of an equation derived by us previously using a canonical transformation in the TC plus normal-metal Fermi sea problem (see Eq. (8) in Ref. 17).

It is instructive to derive a sum rule for the noise spectrum starting from Eq. (23). First, note that the TC occupation number and TC pairing correlator are related to the spectral functions in the following way,

$$\bar{n}_\sigma=\langle d^\dagger_\sigma d_\sigma\rangle=\int d\epsilon'\mathcal{A}(\epsilon')f(\epsilon'), \tag{25a}$$

$$F_d=-\langle d_\uparrow d_\downarrow\rangle=\int d\epsilon'\mathcal{B}(\epsilon')f(\epsilon'). \tag{25b}$$

Equation (25b) shows that the spectral function $\mathcal{B}(\epsilon')$ describes the extent to which TC pairing is induced through its hybridization with the Fermi gas, i.e., $\mathcal{B}(\epsilon')$ can be inter-

preted as a single-state proximity effect. Integrating Eq. (23) over all frequencies and using Eqs. (25a) and (25b) we obtain the following sum rule,

$$\langle(\delta\hat{n})^2\rangle = \int_{-\infty}^{\infty} \tilde{S}_n(\omega)d\omega = \sum_{\sigma} [\bar{n}_\sigma(1-\bar{n}_\sigma) + F_d^2]. \quad (26)$$

As a cross check, Eq. (26) can be derived directly without using Eq. (23) by simple applications of Wick's theorem and use of the Fermi anticommutation relation, such that $\hat{n}_\sigma^2 = \hat{n}_\sigma$. Interestingly, the sum rule [Eq. (26)] shows that the onset of superconductivity tends to *increase* the amount of noise produced by a TC.

V. TRAPPING-CENTER SPECTRAL DENSITIES AND ANDREEV BOUND STATES

The TC spectral densities are known exactly for the case of zero on-site Coulomb repulsion.[42–44] These can be written as

$$\mathcal{A} = A\,\theta(|\epsilon| - \Delta) + [a_+\delta(\epsilon - E_b) + a_-\delta(\epsilon + E_b)], \quad (27a)$$

$$\mathcal{B} = B\,\theta(|\epsilon| - \Delta) + b_+[\delta(\epsilon - E_b) - \delta(\epsilon + E_b)], \quad (27b)$$

where θ is the step function. Each spectral density is composed of a continuous above-gap component which is nonzero only at energies outside the superconducting gap ($|\epsilon| > \Delta$). For energies within the gap, there are two sharp Andreev bound states, with positive particlelike energy E_b and negative holelike energy $-E_b$. These bound states are reminiscent of the TC localized level ϵ_d, whose energy is renormalized to $\pm E_b$ due to hybridization with Cooper pairs.

In order to express these functions analytically, we define the trap hybridization parameter γ as

$$\gamma = \pi g_0 \langle V_k^2 \rangle_{\epsilon_k = \epsilon_F}, \quad (28)$$

where V_k is averaged over $\epsilon_k = \epsilon_F$ and g_0 is the energy density at the Fermi level. The above-gap contributions are given by

$$A(\epsilon) = \frac{\gamma|\epsilon|\sqrt{\epsilon^2 - \Delta^2}[(\epsilon + \epsilon_d)^2 + \gamma^2]}{\pi(\epsilon^2 - \Delta^2)[(\epsilon^2 + \epsilon_d^2 + \gamma^2)^2 - (2\epsilon\epsilon_d)^2] + (2\epsilon\Delta\gamma)^2}, \quad (29a)$$

$$B(\epsilon) = \frac{-\,\mathrm{sgn}(\epsilon)\gamma\Delta\sqrt{\epsilon^2 - \Delta^2}[\epsilon^2 - \epsilon_d^2 - \gamma^2]}{\pi(\epsilon^2 - \Delta^2)[(\epsilon^2 + \epsilon_d^2 + \gamma^2)^2 - (2\epsilon\epsilon_d)^2] + (2\epsilon\Delta\gamma)^2}, \quad (29b)$$

where $\mathrm{sgn}(\epsilon)$ denotes the sign of ϵ. We remark that these are finite-temperature spectral densities; the temperature does not appear explicitly because the Matsubara Green's functions for $U=0$ depend on temperature only through the Matsubara frequencies.[42] The Andreev bound-state energy is given by the single pair of real roots $\pm E_b$ of

$$E^2\left(1 + \frac{2\gamma}{\sqrt{\Delta^2 - E^2}}\right) - \epsilon_d^2 - \gamma^2 = 0, \quad (30)$$

with the amplitudes $a_\pm$ and b_+ of Eqs. (27a) and (27b) given by

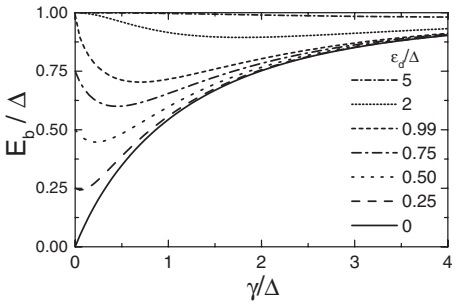

FIG. 2. Particlelike Andreev bound state as a function of hybridization γ for different trap energies ϵ_d, all in units of the superconducting gap Δ. The holelike Andreev bound state has the same energy but opposite sign.

$$a_\pm = \frac{(\Delta^2 - E_b^2)[(\epsilon_d \pm E_b)^2 + \gamma^2]}{2[(2\Delta^2 - E_b^2)(\epsilon_d^2 + \gamma^2) - E_b^4]}, \quad (31a)$$

$$b_+ = \frac{-\,\gamma\Delta E_b\sqrt{\Delta^2 - E_b^2}}{[(2\Delta^2 - E_b^2)(\epsilon_d^2 + \gamma^2) - E_b^4]}. \quad (31b)$$

Note that $a_+ \neq a_-$ in the asymmetric case $\epsilon_d \neq 0$ but $b_+ = b_-$ always. A useful relation is that $b_+ = -\sqrt{a_+ a_-}$. In Fig. 2 we plot the Andreev levels E_b as a function of TC hybridization for different TC energies ϵ_d.

It is useful to establish a connection to the case of a point contact between superconductors.[45] In this case the transmission of electrons across the point contact is dominated by the presence of two Andreev bound states at equal and opposite energies with respect to the Fermi level. For zero phase difference these Andreev levels are located close to $\pm\Delta$. In our case, the trapping center is equivalent to a point contact provided $|\epsilon_d| \gg \Delta$; looking at Fig. 2 we see that E_b is indeed slightly below Δ in this limit.

VI. EXPLICIT RESULTS FOR THE NOISE SPECTRUM

We now show explicit results for the noise spectrum of a single TC hybridized with a superconductor. The analytic expressions for the spectral functions are inserted into Eq. (23), where in the absence of a magnetic field $\Sigma_{\sigma,\sigma'} = 2$ and $\mathcal{A}_{\sigma-\sigma} = \mathcal{B}_{\sigma\sigma} = 0$. For $\omega \geq 0$ the noise is given by

$$\tilde{S}_n(\omega) = 2\hbar\left\{\left[\int_{-\infty}^{-\Delta} + \int_{\Delta+\omega}^{\infty} + \theta(\omega - 2\Delta)\int_{\Delta}^{-\Delta+\omega} d\epsilon\right]\right.$$
$$\times[A(\epsilon)A(\epsilon - \omega) - B(\epsilon)B(\epsilon - \omega)][1 - f(\epsilon)]f(\epsilon - \omega) \quad (32a)$$

$$+ 2a_+a_-[1 - f(E_b)]f(-E_b)\delta(\omega - 2E_b) \quad (32b)$$

$$+ \sum_{\xi=+,-} \theta(\omega - \xi E_b - \Delta)[a_\xi A(\xi E_b - \omega)$$
$$+ a_{-\xi}A(-\xi E_b + \omega) - 2b_+B(\xi E_b - \omega)]$$
$$\left.\times[1 - f(\xi E_b)]f(\xi E_b - \omega)\right\}. \quad (32c)$$

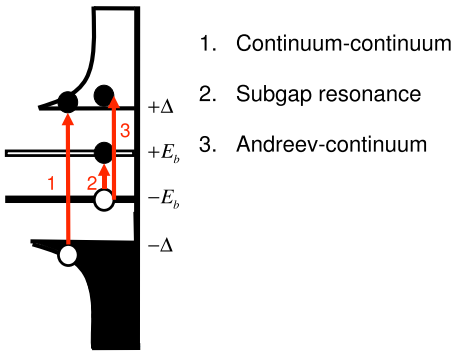

FIG. 3. (Color online) Depiction of the energy density as a function of energy for the TC plus superconductor model and the most important quasiparticle-quasihole excitations (denoted by arrows) determining the TC noise spectrum.

The $\omega<0$ expression can be obtained from detailed balance $\tilde{S}(-\omega)=e^{-\hbar\omega/k_BT}\tilde{S}(\omega)$.

The positive frequency spectrum is interpreted as the sum over all possible quasiparticle-quasihole pairs created when the TC plus Fermi sea absorbs a photon with energy $\hbar\omega$ emitted by the noise detector. Figure 3 illustrates the energy excitations associated to TC noise. The first contribution is a continuum-continuum transition Eq. (32a) where the hole (particle) is in the continuum below (above) the superconducting gap. This gives a smooth contribution to the noise spectrum when $\omega>2\Delta$. The second line Eq. (32b) is the *subgap resonance*. The resonance occurs when a hole is created at Andreev level $-E_b$ and a particle is excited at level $+E_b$. This contribution is a sharp transition between Andreev levels: the noise is a delta-function peaked at $\omega=2E_b$. The third line Eq. (32c) refers to transitions involving one of the Andreev levels and the continuum. This gives smooth contributions for $\omega>\Delta\pm E_b$.

Figure 4 shows the noise spectrum for temperatures above and below the critical temperature for transition into the superconducting state. We assume $\epsilon_d=0$, with the superconducting energy gap dependent on temperature according to

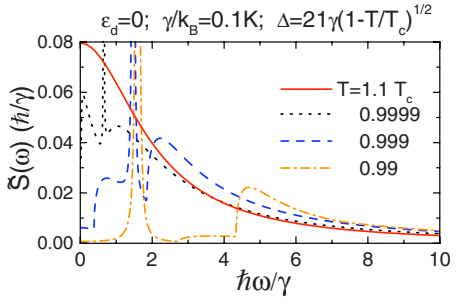

FIG. 4. (Color online) Trapping-center noise spectrum near the superconducting transition temperature T_c, for $\epsilon_d=0$. For $T>T_c$ the noise has the Lorentzian form characteristic of random telegraph noise (Ref. 17). As T is lowered below T_c a gap opens in the noise spectrum, and a sharp subgap resonance appears as a transition between two Andreev bound states (for convenience, we represent the subgap resonance with a phenomenological linewidth equal to 0.01γ). This shows that TC noise is dramatically affected by superconductivity.

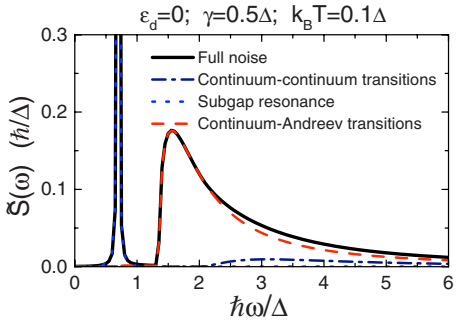

FIG. 5. (Color online) Trapping-center noise for temperatures well below the superconducting transition. The parameters are $\gamma=0.5\Delta$, $\epsilon_d=0$, $k_BT=0.1\Delta$, leading to Andreev energy $E_b=0.35\Delta$. About 60% of the noise power is due to one sharp subgap resonance represented here by a Lorentzian with linewidth 0.001Δ. The remaining 40% is dominated by processes involving the creation of a hole in the continuum and the excitation of an Andreev level at $+E_b$. This occurs only for $\omega>\Delta+E_b$.

$\Delta=1.76k_BT_c\sqrt{1-T/T_c}$ for $T\leq T_c$ and $\Delta=0$ for $T>T_c$.[33] We assumed $k_BT_c/\gamma=11.96$, consistent with the value of $T_c=1.196$ K for aluminum with a trap hybridization parameter $\gamma/k_B=0.1$ K. For $T>T_c$ the noise is a Lorentzian with linewidth $2\gamma/\hbar$, consistent with the high-temperature limit for random telegraph noise discussed in Ref. 17 (note that $k_BT_c\gg\gamma$ in Fig. 4). As the temperature is lowered below T_c a sharp resonance appears at energy equal to two E_b. To display the subgap resonance in the figure we represented the delta function as a Lorentzian with linewidth equal to 0.01γ.

For $T\ll T_c$, $k_BT\ll E_b$, and $\epsilon_d\lesssim\Delta$ the noise is well approximated by

$$\tilde{S}_n(\omega)\approx 2\hbar\{2a_+a_-\delta(\omega-2E_b)+\theta(\omega-E_b-\Delta)\times[a_+A(E_b-\omega)+a_-A(-E_b+\omega)-2b_+B(E_b-\omega)]\}. \quad (33)$$

Figure 5 shows the low-temperature noise spectrum ($T\ll T_c$) with parameters normalized by the superconducting energy gap. We also show the breakdown of the noise into its various contributions. For convenience, we represented the subgap resonance as a Lorentzian with linewidth 0.001Δ. Our theory does not account for broadening mechanisms but we expect that disorder and other inhomogeneities will be a source of broadening for Andreev bound states.

For the parameters of Fig. 5 the subgap resonance accounts for 59% of the noise power. The remainder is due to Andreev-continuum transitions (33%) with continuum-continuum transitions contributing only 8%. Remarkably, the continuum-continuum contribution is quite small, in spite of being responsible for *all* the Lorentzian noise at $T>T_c$ (in the normal state).

Figure 6 shows the low-temperature noise spectrum for a case where the Andreev bound states are very close to the gap edge, $E_b=0.981\Delta$ (parameters $\epsilon_d=0$, $\gamma=10\Delta$, and $k_BT=0.1\Delta$). This case is quite different from Fig. 5: the continuum-continuum contribution is now 94% of the noise power, with Andreev-continuum contributions 5.7%, and subgap resonance contributing only 0.3%.

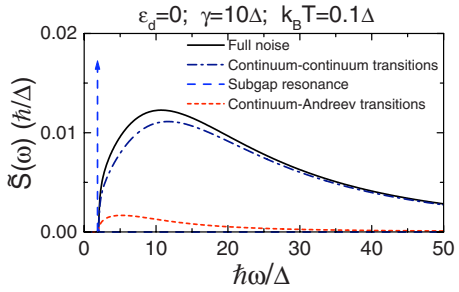

FIG. 6. (Color online) TC noise spectrum in the superconducting regime in a case where the Andreev bound states are very close to the gap edge (E_b=0.981Δ). Here the noise is dominated by continuum-continuum contributions (94% of the noise power) with the subgap resonance contributing only 0.3%.

Figure 7 depicts the noise in the asymmetric regime ($\epsilon_d \neq 0$) with ϵ_d=5Δ, γ=0.5Δ, and k_BT=0.1Δ (the Andreev bound states are at E_b=0.999Δ). Here the continuum-continuum contribution accounts for 98% of the noise, with Andreev-continuum transitions contributing ≈2% and subgap resonance contributing less than 0.1%. Interestingly, the noise has a broad peak at $\hbar\omega$=6Δ, that occurs because the spectral functions have a smooth peak at ϵ_d=5Δ. Figures 5–7 show that the noise changes its character *completely* due to the opening of a gap and the formation of Andreev bound states in a superconductor.

VII. ANDREEV STATES AS JUNCTION RESONATORS

We now relate our theory to the experimental observation of "spurious two-level systems" (microresonators) in phase-based[6] and flux-based[8] superconducting qubits. The model Hamiltonian for the interaction of a qubit with a TC plus Fermi sea is simplified by projecting onto the Hilbert space of Andreev bound states. This is achieved by expressing the TC operators as

$$d_\uparrow = u\left(\frac{\alpha_-^\dagger + \alpha_+}{\sqrt{2}}\right) + v\left(\frac{\alpha_- - \alpha_+^\dagger}{\sqrt{2}}\right) + d_{\uparrow,\mathrm{cont}}, \tag{34a}$$

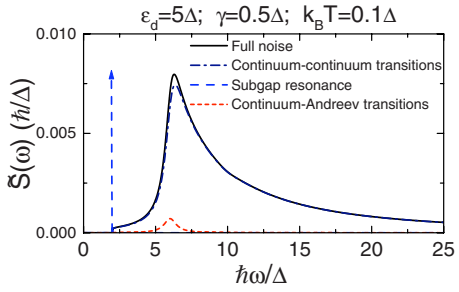

FIG. 7. (Color online) TC noise spectrum for the asymmetric case ϵ_d=5Δ with Andreev levels at $\pm E_b = \pm 0.999\Delta$. The noise spectra has a smooth peak close to $\hbar\omega$=6Δ. This occurs because the spectral function peaks at ϵ_d. Similar to Fig. 6, the noise is dominated by continuum-continuum contributions (98%) with the subgap resonance contributing less than 0.1%.

$$d_\downarrow^\dagger = -v\left(\frac{\alpha_-^\dagger + \alpha_+}{\sqrt{2}}\right) + u\left(\frac{\alpha_- - \alpha_+^\dagger}{\sqrt{2}}\right) + d_{\downarrow,\mathrm{cont}}, \tag{34b}$$

where $\alpha_\pm^\dagger$ is a creation operator for an Andreev level with energy $\pm E_b$ and the $d_{\sigma,\mathrm{cont}}$ denote the additional operators acting on the continuum. The canonical transformation defined by Eqs. (34a) and (34b) diagonalizes our TC model when $u=\sqrt{a_+}$ and $v=\sqrt{a_-}$. This can be verified by calculating the Green's function using the canonical transformation and comparing to Eqs. (27a) and (27b). Substituting Eqs. (34a) and (34b) into Eq. (2) we get an effective Hamiltonian for the qubit interacting with a pair of Andreev bound states,

$$\mathcal{H}_{Q\text{-A}} = \frac{1}{2}\hbar\Omega_0\hat{\sigma}_z + E_b\alpha_+^\dagger\alpha_+ - E_b\alpha_-^\dagger\alpha_- + (\lambda_z\hat{\sigma}_z + \lambda_x\hat{\sigma}_x) \times [2\sqrt{a_+a_-}(\alpha_+^\dagger\alpha_- + \alpha_-^\dagger\alpha_+) + (a_+ - a_-)(\alpha_+^\dagger\alpha_+ - \alpha_-^\dagger\alpha_-)]. \tag{35}$$

Here $\lambda_z=\hbar(\delta I_c)\eta_z$ and $\lambda_x=\hbar(\delta I_c)\eta_x$ are characteristic coupling energies between the qubit and the Andreev levels. For phase qubits these should be a fraction of the change in Josephson energy $\hbar(\delta I_c)/(2e)$. Recall from Sec. II that the η's depend on qubit design while (δI_c) is the characteristic shift in critical current due to a TC. A similar expression will hold for other kinds of qubits, for example, in a Cooper-pair box $\lambda_i \sim p_Q p_{\mathrm{TC}}/R^3$ is the electrostatic energy due to the interaction of the qubit's electric dipole moment p_Q and the TC (dipole moment p_{TC} due to the image charge produced at the reservoir).[17]

The qubit-Andreev interaction is weighted by additional factors accounting for the branching of the impurity spectral weight into different channels—not all of the impurity's noise goes into the Andreev channel. The first interaction, $2\sqrt{a_+a_-}(\alpha_+^\dagger\alpha_- + \alpha_-^\dagger\alpha_+)(\lambda_z\hat{\sigma}_z + \lambda_x\hat{\sigma}_x)$ produces admixture between qubit and Andreev levels, and leads to important anticrossings in qubit spectrometry. The second interaction, $(a_+ - a_-)(\alpha_+^\dagger\alpha_+ - \alpha_-^\dagger\alpha_-)(\lambda_z\hat{\sigma}_z + \lambda_x\hat{\sigma}_x)$ only exists in the asymmetric case ($\epsilon_d \neq 0$). It enables the design of quantum gates through electrical manipulation of Andreev states.

Hamiltonian (35) describes a four-level system, where the qubit energy levels are hybridized with the pair of Andreev states; it serves as a starting point to study nonequilibrium effects for a qubit coupled to Andreev excitations. Figure 8(a) shows the energy levels E_i obtained after diagonalizing Eq. (35) for $\lambda_x=0.2E_b$ and $\lambda_z=0$. Note the level anticrossing when $\hbar\Omega_0=2E_b$. Figure 8(b) shows the two lowest energy transitions measured by qubit spectroscopy, E_1-E_0 and E_2-E_0. We remark the similarity of our Fig. 8(b) to the experimental data in Fig. 2(a) of Ref. 6. For these frequencies the qubit is highly mixed with the Andreev excitation.

Therefore each pair of Andreev levels acts as a microresonator with frequency in the range $2E_b \in (0, 2\Delta)$. The anticrossing behavior occurs only when the qubit is in resonance with a transition between Andreev levels, i.e., when the qubit frequency coincides with a subgap resonance in the noise spectrum.

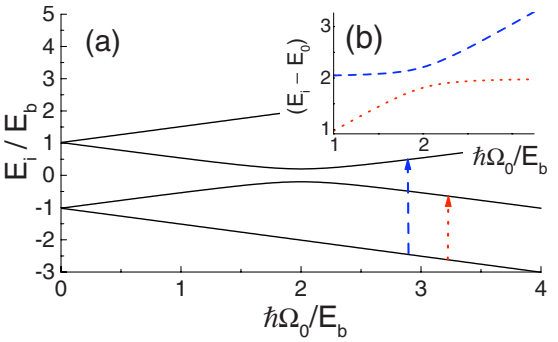

FIG. 8. (Color online) (a) Energy-level structure of the effective Hamiltonian for a superconducting qubit interacting with a pair of Andreev bound states (one holelike at energy $-E_b$ and one particlelike at $+E_b$). The Andreev-qubit coupling is assumed $\lambda=0.2E_b$. Anticrossing behavior occurs when the qubit energy splitting matches the subgap resonance, $\hbar\omega=2E_b$. (b) Energy differences between the ground state and the first and second excited states. The result is remarkably similar to spectroscopy measurements on phase (Ref. 6) and flux qubits (Ref. 8).

VIII. DISCUSSION AND CONCLUSION

In summary, we calculated the noise spectrum due to individual TCs hybridized with a superconducting lead. We showed that the opening of a gap and the formation of Andreev bound states change the character of the noise completely. At $T<T_c$, the noise is substantially different from the usual Lorentzian spectra assumed in simple models.

In many cases the noise is dominated by a subgap resonance related to transitions between Andreev bound states at energies $\pm E_b$ reminiscent of the localized TC states. At $T \ll T_c$, the subgap resonance may account for over half of the noise power (see Fig. 5). The remaining noise power occurs only at $\hbar\omega>\Delta+E_b$, giving a smooth gapped spectrum related to the excitation of an Andreev level into the continuum.

We assumed a TC model with zero on-site Coulomb repulsion. As a result, the noise can be expressed exactly as an integral over TC spectral densities, which are known analytically. This constitutes a limiting case which provides a fully characterized reference point. We now discuss the expected role of TC Coulomb repulsion. Spectral densities for $U>0$ were calculated using the numerical renormalization group method in Refs. 43 and 44. For $U>0$, the energy E_b of each Andreev level is shifted but the number of Andreev levels remains the same (one holelike and one particlelike per TC).[43,44]

At $U=0$, the total noise power [Eq. (26)] is appreciable only if ϵ_d lies within the interval $[-\Delta,\Delta]$ (or within $\mathrm{Max}\{k_BT,\gamma\}$ of this interval. For $T>T_c$ this result is equivalent to the one found in Ref. 17). An interesting open question is whether this result will change for $U>0$.

We derived an effective Hamiltonian for a superconducting qubit interacting with a TC, showing that the qubit sees the TC as two Andreev levels. Anticrossing occurs when the qubit frequency is in resonance with the energy separation of the two Andreev levels. This gives a microscopic explanation for the experimental observation of microresonators coupled to Josephson-junction devices. Simmonds *et al.*[6] observed anticrossing behavior at a number of frequencies in the spectroscopy of Josephson-junction phase qubits.[7] Plourde *et al.*[8] observed a similar effect in the spectroscopy of flux qubits. Kim *et al.*[46] observed avoided level crossings in the spectra of a Cooper-pair box. Our work establishes a direct connection between TCs in the Josephson-junction insulator and the presence of these anticrossings.

Another interesting implication of our model is that each TC will become a sharp dielectric resonance *only* when the lead becomes a superconductor. TCs are charged defects, possessing an electric dipole moment due to their image charge in the superconducting lead. The fluctuation-dissipation theorem implies that the power absorbed by a TC irradiated by an ac electric field at frequency ω is given by $P_\omega \propto \omega\tilde{S}_n(\omega)$. Therefore, the subgap resonance in $\tilde{S}_n(\omega)$ can be detected as a sharp resonance in dielectric absorption P_ω (in the normal state, P_ω will be a broad resonance, see Fig. 4).

This effect provides a powerful method to validate our theory experimentally. There are two other microscopic models for the microresonator: macroscopic resonant tunneling[14] results in no dielectric resonance; structural two-level system[10,15] gives rise to the *same* dielectric resonance above and below T_c. Hence microwave absorption experiments above and below T_c will clearly reveal whether the microresonator is a pair of Andreev levels or not.

In conclusion, we have developed a microscopic theory for critical current and charge noise in superconducting devices based on a charge tunneling model with individual trapping centers. We showed that the superconducting gap and the formation of Andreev levels plays a prominent role in determining the noise spectrum, providing a microscopic explanation for the microresonators observed in experiments. Our calculated noise spectrum is drastically different from the usual phenomenological Lorentzian and $1/f$ noise spectra derived in previous work.

ACKNOWLEDGMENTS

R.d.S. and F.K.W. acknowledge support from NSERC-Discovery. R.d.S also acknowledges support from the University of Victoria Faculty of Sciences. T.H. and J.v.D. acknowledge support from the DFG through Grants No. SFB631 and No. SFB-TR12, and the German Excellence Initiative via the "Nanosystems Initiative Munich (NIM)," as well as partial support from DIP-H.2.1, and from the NSF under Grant No. NSF PHY05-51164.

[1] D. J. Van Harlingen, T. L. Robertson, B. L. T. Plourde, P. A. Reichardt, T. A. Crane, and J. Clarke, Phys. Rev. B **70**, 064517 (2004).
[2] F. C. Wellstood, C. Urbina, and J. Clarke, Appl. Phys. Lett. **85**, 5296 (2004).
[3] G. Ithier, E. Collin, P. Joyez, P. J. Meeson, D. Vion, D. Esteve, F. Chiarello, A. Shnirman, Y. Makhlin, J. Schriefl, and G. Schön, Phys. Rev. B **72**, 134519 (2005).
[4] R. T. Wakai and D. J. Van Harlingen, Phys. Rev. Lett. **58**, 1687 (1987); B. Savo, F. C. Wellstood, and J. Clarke, Appl. Phys. Lett. **50**, 1757 (1987).
[5] Sh. Kogan, *Electronic Noise and Fluctuations in Solids* (Cambridge University Press, Cambridge, UK, 1996).
[6] R. W. Simmonds, K. M. Lang, D. A. Hite, S. Nam, D. P. Pappas, and J. M. Martinis, Phys. Rev. Lett. **93**, 077003 (2004).
[7] K. B. Cooper, M. Steffen, R. McDermott, R. W. Simmonds, S. Oh, D. A. Hite, D. P. Pappas, and J. M. Martinis, Phys. Rev. Lett. **93**, 180401 (2004).
[8] B. L. T. Plourde, T. L. Robertson, P. A. Reichardt, T. Hime, S. Linzen, C.-E. Wu, and J. Clarke, Phys. Rev. B **72**, 060506(R) (2005).
[9] S. Oh, K. Cicak, J. S. Kline, M. A. Sillanpaa, K. D. Osborn, J. D. Whittaker, R. W. Simmonds, and D. P. Pappas, Phys. Rev. B **74**, 100502(R) (2006).
[10] J. M. Martinis, K. B. Cooper, R. McDermott, M. Steffen, M. Ansmann, K. D. Osborn, K. Cicak, S. Oh, D. P. Pappas, R. W. Simmonds, and C. C. Yu, Phys. Rev. Lett. **95**, 210503 (2005).
[11] I. Martin, L. Bulaevskii, and A. Shnirman, Phys. Rev. Lett. **95**, 127002 (2005).
[12] L. Tian and R. W. Simmonds, Phys. Rev. Lett. **99**, 137002 (2007).
[13] A. Shnirman, G. Schön, I. Martin, and Yu. Makhlin, Phys. Rev. Lett. **94**, 127002 (2005).
[14] P. R. Johnson, W. T. Parsons, F. W. Strauch, J. R. Anderson, A. J. Dragt, C. J. Lobb, and F. C. Wellstood, Phys. Rev. Lett. **94**, 187004 (2005).
[15] M. Constantin and C. C. Yu, Phys. Rev. Lett. **99**, 207001 (2007).
[16] A. M. Zagoskin, S. Ashhab, J. R. Johansson, and Franco Nori, Phys. Rev. Lett. **97**, 077001 (2006).
[17] R. de Sousa, K. B. Whaley, F. K. Wilhelm, and J. von Delft, Phys. Rev. Lett. **95**, 247006 (2005).
[18] L. Faoro, J. Bergli, B. L. Altshuler, and Y. M. Galperin, Phys. Rev. Lett. **95**, 046805 (2005).
[19] L. Faoro and L. B. Ioffe, Phys. Rev. Lett. **96**, 047001 (2006); L. Faoro, A. Kitaev, and L. B. Ioffe, *ibid.* **101**, 247002 (2008).
[20] R. M. Lutchyn, Ł. Cywiński, C. P. Nave, and S. Das Sarma, Phys. Rev. B **78**, 024508 (2008).
[21] A. B. Zorin, F. J. Ahlers, J. Niemeyer, T. Weimann, H. Wolf, V. A. Krupenin, and S. V. Lotkhov, Phys. Rev. B **53**, 13682 (1996).
[22] Y. Nakamura, Yu. A. Pashkin, T. Yamamoto, and J. S. Tsai, Phys. Rev. Lett. **88**, 047901 (2002).
[23] O. Astafiev, Yu. A. Pashkin, Y. Nakamura, T. Yamamoto, and J. S. Tsai, Phys. Rev. Lett. **93**, 267007 (2004).
[24] T. Hayashi, T. Fujisawa, H. D. Cheong, Y. H. Jeong, and Y. Hirayama, Phys. Rev. Lett. **91**, 226804 (2003); J. R. Petta, A. C. Johnson, C. M. Marcus, M. P. Hanson, and A. C. Gossard, *ibid.* **93**, 186802 (2004); J. Gorman, D. G. Hasko, and D. A. Williams, *ibid.* **95**, 090502 (2005).
[25] M. R. Buitelaar, T. Nussbaumer, and C. Schönenberger, Phys. Rev. Lett. **89**, 256801 (2002); Y. Avishai, A. Golub, and A. D. Zaikin, Europhys. Lett. **55**, 397 (2001).
[26] W. Lu, Z. Ji, L. Pfeiffer, K. W. West, and A. J. Rimberg, Nature (London) **423**, 422 (2003).
[27] J. Clarke and F. K. Wilhelm, Nature (London) **453**, 1031 (2008).
[28] J. M. Martinis, S. Nam, J. Aumentado, K. M. Lang, and C. Urbina, Phys. Rev. B **67**, 094510 (2003).
[29] R. de Sousa, Top. Appl. Phys. **115**, 183 (2009).
[30] F. K. Wilhelm, New J. Phys. **10**, 115011 (2008).
[31] R. J. Schoelkopf, A. A. Clerk, S. M. Girvin, K. W. Lehnert, and M. H. Devoret, in *Quantum Noise*, edited by Yu. V. Nazarov and Ya. M. Blanter (Kluwer, Dordrecht, 2002).
[32] P. W. Anderson, Phys. Rev. **124**, 41 (1961).
[33] M. Tinkham, *Introduction to Superconductivity* (Dover, New York, 2004).
[34] B. D. Josephson, in *Superconductivity* Vol. I, edited by R. D. Parks (M. Dekker, New York, USA, 1969), Chap. 9.
[35] V. Ambegaokar, U. Eckern, and G. Schön, Phys. Rev. Lett. **48**, 1745 (1982).
[36] J. Eroms, L. C. van Schaarenburg, E. F. C. Driessen, J. H. Planternberg, C. M. Huizinga, R. N. Schouten, A. H. Verbruggen, C. J. P. M. Harmans, and J. E. Mooij, Appl. Phys. Lett. **89**, 122516 (2006).
[37] L. I. Glazman and K. A. Matveev, JETP Lett. **49**, 659 (1989).
[38] M.-S. Choi, M. Lee, K. Kang, and W. Belzig, Phys. Rev. B **70**, 020502(R) (2004).
[39] G. Heinrich and F. K. Wilhelm, arXiv:0808.3705 (unpublished).
[40] G. B. Lesovik and R. Loosen, JETP Lett. **65**, 295 (1997).
[41] See A. L. Fetter and J. D. Walecka, *Quantum Theory of Many-Particle Systems* (McGraw-Hill, Boston, USA, 1971), Secs. 23, 24, 32, and 51.
[42] T. Yoshioka and Y. Ohashi, J. Phys. Soc. Jpn. **69**, 1812 (2000).
[43] J. Bauer, A. Oguri, and A. C. Hewson, J. Phys.: Condens. Matter **19**, 486211 (2007).
[44] T. Hecht, A. Weichselbaum, J. von Delft, and R. Bulla, J. Phys.: Condens. Matter **20**, 275213 (2008).
[45] M. F. Goffman, R. Cron, A. Levy Yeyati, P. Joyez, M. H. Devoret, D. Esteve, and C. Urbina, Phys. Rev. Lett. **85**, 170 (2000).
[46] Z. Kim, V. Zaretskey, Y. Yoon, J. F. Schneiderman, M. D. Shaw, P. M. Echternach, F. C. Wellstood, and B. S. Palmer, Phys. Rev. B **78**, 144506 (2008).